

The Energy Criteria for Elastic-Plastic Fracture in Tough Paper^{*1}

Jong-Moon Park^{*2} · James Thorpe^{*3}

고인성 종이의 탄성-소성 파괴의 에너지 판단기준^{*1}

박 종 문^{*2} · James Thorpe^{*3}

요 약

고인성 종이의 탄성-소성 파괴를 파괴역학을 이용하여 분석하였다. 탄성-소성 물질의 파괴에 있어서 균열이 언제 진행되기 시작하는지 이론적 판단 기준을 유도하고, mode I 파괴를 linear image strain analysis(LISA)로 관찰한 후, 파괴역학 변수들을 계산하였다. 크랙(crack)이 있는 물질에 외부하중이 작용할때 변형률 에너지를 발산 속도(strain energy release rate)가 그 물질이 견딜 수 있는 파괴저항(fracture resistance)에 도달하면 안정적인 파괴가 진행된다. 이를 이용하여 크랙의 초기 진행시 결점주위의 응력, 파괴저항, 크랙 진행거리, 기하인자(geometry factor) 등을 구하였다. 이 변수들은 종이의 파괴역학적 특성을 정량적으로 나타내므로 유용하게 활용될 수 있을 것이다.

Keywords : Fracture criteria, elastic-plastic fracture, tough paper, mode I, fracture parameters

1. INTRODUCTION

Many uses of paper require application of a service load high enough to initiate cracks, particularly when pre-existing flaws or stress concentrations are present in the sheet. Manufacturing processes involving drawing of the wet web also introduces cracks that may continue to grow until the residual strength of the sheet becomes so low that fracture occurs. Mode

I fracture testing presents a convenient method to analyze the tensile failure of paper or any material with cracks or flaws within its structure (Choi & Thorpe, 1991; Choi, *et al.*, 1991; Steadman & Fellers, 1986 · 1987; Park, 1993). Mode I fracture analysis allows attention to be focused on the tip of an induced crack for experimental analysis, but extension of the concept to inherent cracks or flaws within the paper is easy to see.

1. 접수 1996 10월 30일 Received October 30, 1996

2. 충북대학교 산림과학부 School of Forest Resources, Chungbuk National University, Cheongju 361-763, Korea

3. 미국 뉴욕주립대학 College of Environmental Science & Forestry, State Univ. of New York, Syracuse, NY 13210, USA

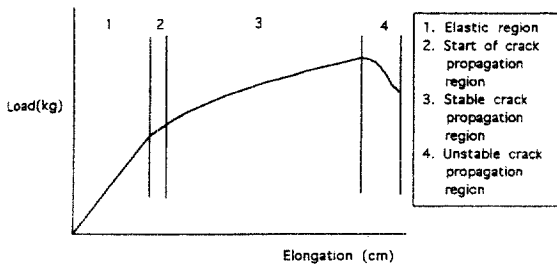


Fig. 1. Four regions of the load-elongation curve.

In this study, application of fracture mechanics theory to a paper is attempted. The application method may need to be refined, but with linear image strain analysis (LISA) indicate that many of the fracture mechanics' parameters meet expectation.

Mode I tensile specimen load-elongation curves can be separated into four regions. The initial high modulus elastic region of the curve allows for elastic stretching of the paper and a blunting of the crack tip. The second region is a transition to a lower modulus region that marks the start of crack propagation. The third region of decreasing modulus is a region of slow stable crack growth. The fourth region is unstabled crack growth followed by failure. Each of these regions is shown in Fig. 1. During crack propagation in tough paper the disproportional plastic deformation at the tip of the spreading crack is quite different from the deformation of the stationary crack. The irreversible plastic strains near the crack tip diverge as the crack propagates causing additional deformation of the material in order to maintain an adequate strain field at the extending crack tip. The additional deformation required to maintain the necessary strain concentration at the propagating crack tip becomes the source of stable crack growth.

The energy criterion of elastic-plastic fracture mechanics (EPFM) will be applied to paper to analyze paper toughness.

1.1 Application of elastic-plastic fracture mechanics to paper

Linear Elastic Fracture Mechanics (LEFM) provides an analysis of fracture based on parameter representing the crack tip stress field. LEFM can be applied to materials with relatively low fracture resistance on the basis of elastic concepts and with small plastic zones compared to the crack size. Elastic-Plastic Fracture Mechanics (EPFM) analyzes fracture in ductile structures containing flaws. For tough paper grades, like kraft sack, photocopy, liner board, and manila folder paper, EPFM should be used because there is considerable plastic deformation during fracture as shown in previous work (Park, 1993).

In metallic materials, a single crack tip opening displacement (CTOD) is measured to test for plastic strain and used as an approximation of crack propagation. For paper, a linear image strain analysis (LISA) method developed at Empire State Paper Research Ins. (ESPRI) gives a direct strain profile of observed area by non-contact image analysis (Choi & Thorpe, 1991; Choi *et al.*, 1991).

Fracture behavior of material like paper can be quite different in the plane strain or plane stress case. When the z-directional stress is zero ($\sigma_z=0$), it is the plane stress case. There is no constraint of deformation in thickness direction in plane stress case. On the other hand, when there is no z-directional strain ($\epsilon_z=0$), it is the plane strain case. In the plane strain case, there is the constraint of deformation in thickness direction. Paper is nearer the plane stress case than the plane strain case. Therefore the plane stress condition is assumed for paper.

In the following sections, a theory of the energy criteria for elastic-plastic fracture is summarized and the energy criterion described graphically. Graphical understanding of the energy criterion allows use of fracture mechanics parameters which characterize fracture behavior and toughness of paper.

1. 1. 1 Theoretical derivation of the energy criteria for elastic-plastic fracture in tough paper

From the energy conservation rule, the fracture criterion is established (Broek, 1989). The fracture criterion is that the strain energy release rate dU/da is the same as the fracture energy or fracture resistance dW/da . Namely, $dU/da=dW/da$ (1). Where, U =strain energy, a =crack length, and W =work applied or required in fracturing material. From eq. (1) according to the energy conservation rule, fracture happens if $(\pi\sigma^2 a/E)=dW/da$ (2). Where, σ =stress, and E =Young's modulus. In other words, fracture occurs when the strain energy release rate, $\pi\sigma^2 a/E$, equals the fracture energy per unit crack extension, dW/da . The fracture energy per unit crack extension dW/da is known as fracture resistance, R . We can measure Young's modulus and the fracture resistance (R). When $\pi\sigma^2 a$ reaches certain known value, namely ER , fracture occurs. This $\pi\sigma^2 a$ term is a square of stress intensity factor, K . The square of the stress intensity factor, K , can be expressed as $\beta^2\pi\sigma^2 a$. Where β is called as a geometry factor that depends on sample geometry. β is used to account for the effect of infinite sample size in the stress of a material with a crack. Therefore, eq. (2) becomes $\beta^2\pi\sigma^2 a/E=dW/da$. Because strain $\epsilon=\sigma/E$, substitution yields $\beta^2\pi\sigma\epsilon a=R$ (3).

Up to this point, the derived energy criterion

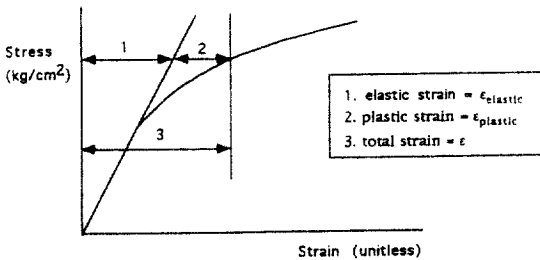


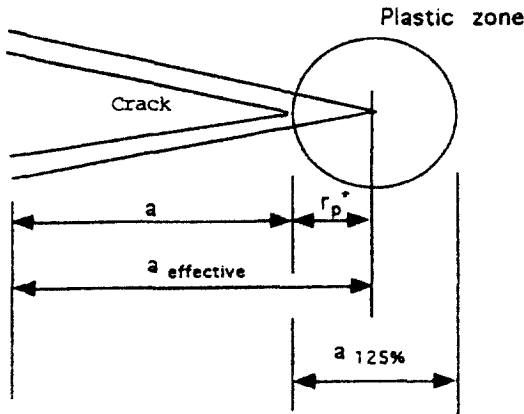
Fig. 2. Classification of strain in a stress-strain curve.

is for LEFM. What follows is for EPFM. In the plastic deformation, the geometry factor β may change. By substitute H for $\beta^2\pi$, the dimensionless geometry factor for plastic deformation, equation (3) becomes $H\sigma\epsilon a=R$ (4). The symbol R is used for the fracture energy of linear-elastic material, J_R is used instead of R for non-linear material. In paper analysis, it is observed that ϵ can be expressed in terms of σ from the empirical equation, in elastic and plastic terms, as a form of Ramberg-Osgood stress-strain equation (Fig. 2).

$\epsilon = \epsilon_{\text{elastic}} + \epsilon_{\text{plastic}} = \sigma/E + \sigma^n/F$ (4). Where, $\epsilon_{\text{elastic}}$ =elastic strain, $\epsilon_{\text{plastic}}$ =plastic strain, and n , F =parameters of the stress-strain curve of the material, which describe the plastic strain. F may be called "pseudo-plastic modulus" because it is located in the denominator as is E , elastic modulus. But F is not a slope of the stress-strain curve as E . The plastic modulus F value is larger than E . Generally when n becomes large then F also becomes large. F has units of $(\text{kgf}/\text{cm}^2)^n$ namely n -th power of stress unit. In the left side term of eq. (3), $\epsilon_{\text{elastic}}$ is expressed as σ/E , then $\beta^2\pi\sigma\epsilon a$ becomes $\pi\beta^2\sigma^2 a/E$. Substituting $\epsilon_{\text{plastic}} = \sigma^n/F$ in eq. (4) provides a $H\sigma^{n+1}a/F$ term. Therefore, eq. (1) becomes $\pi\beta^2\sigma^2 a/E + H\sigma^{n+1}a/F = dW/da$ (5). Strain energy release rate is expressed in elastic and plastic parts. Therefore according to the energy criteria, fracture happens if the strain release rate is equal to the fracture resistance as in the following equation, $\pi\beta^2\sigma^2 a/E + H\sigma^{n+1}a/F = J_R$ (6). The energy criterion of fracture is satisfied when left side terms, $\pi\beta^2\sigma^2 a/E + H\sigma^{n+1}a/F$, which constitutes the J -curve, are equal to the right side term J_R , which constitutes the J_R -curve. The J - and J_R -curve will be described in the following sections in detail.

1. 1. 2 J - and J_R -curve

For a known length of existing crack, the J -curve can be made by substituting stress values into the left side of eq. (6), $J = (\pi\beta^2\sigma^2 a/E) + (H\sigma^{n+1}a/F)$



Where: a = initial crack length,
 $a_{\text{effective}}$ = effective crack length,
 $a_{125\%}$ = size of plastic zone which has
 125% strain of total sample's failure strain,
 r_p^* = radius of plastic zone.

Fig. 3. Calculation of $a_{\text{effective}}$.

a/F). when β , a , E , H , n , and F values are known. When β , a , E , H , n , and F values are unknown, the geometry factor, β , and initial crack length, a , can be obtained readily from sample's geometry. Young's modulus, E , stress-strain parameters, n , and F can be calculated from the stress-strain relationship of the material. The geometry factor H can be calculated by two methods which will be described in later section.

The fracture resistance, J_R , represents the material's fracture resistance as toughness. The crack resistance curve for non-linear materials is called the J_R -curve, which can be measured by the area under a load elongation curve divided by specimen thickness and ligament length, $J_R = (2 \times \text{Area}) / (\text{thickness} \times \text{ligament length})$. Effective crack length, $a_{\text{effective}}$, is also needed for J_R -curve. There are two methods to obtain $a_{\text{effective}}$. The first method is measurement with LISA directly, and the second is a theoretical calculation. In this study direct measurement by LISA was used. The effective crack length, $a_{\text{effective}}$, is obtained from the measured crack

propagation length that has 125% of total specimen failure strain by LISA directly. Theoretical method to calculate $a_{\text{effective}}$ (Kumar *et al.*, 1981) is also available. Fig. 3 shows the difference between the initial crack length, a , the effective crack length, $a_{\text{effective}}$, a calculated term, and, $a_{125\%}$, the experimentally measured crack length. The circular plastic zone shown is a first approximation used in the theory. Accommodation between the evolving theory and the initial experimental results will need to be made in the future. However, at this time $a_{\text{effective}}$ has been set equal to the initial crack length, a , plus r_p^* . The term r_p^* represents the theoretical "radius of the plastic zone" which can now be quantified experimentally with current LISA measurements.

1.1.3 Intercept of the crack tip blunting line with curve to get J_{1c}

The J_R value at initial crack propagation is called a critical value of fracture resistance for crack extension, J_{1c} , where subscript 1 means plane stress case and c means critical value. J_{1c} can be obtained by constructing the J_R -curve with a crack tip blunting line. The crack tip blunting line is an extrapolated line (Broek, 1986), which is known as $J_R = 2\sigma_{ys}\Delta a$. The crack tip blunting line is calculated after measuring the yield stress, σ_{ys} , from stress-strain curve by the 0.2%-offset method.

1.1.4 Understanding of J-curve and J_R -curve with the crack tip blunting line

The energy criteria states that the fracture occurs when the energy release rate equals the fracture resistance. That means that when the J-curve and the J_R -curve intercepts graphically after the crack tip blunting line, fracture begins. In Fig. 4, when a stress is σ_1 , $J < J_R$, according to the energy criterion, there is no fracture at point A. When the stress becomes σ_2 , $J = J_R$, there is a crack tip blunting at point B. When the stress becomes σ_3 , there is a crack initiation at

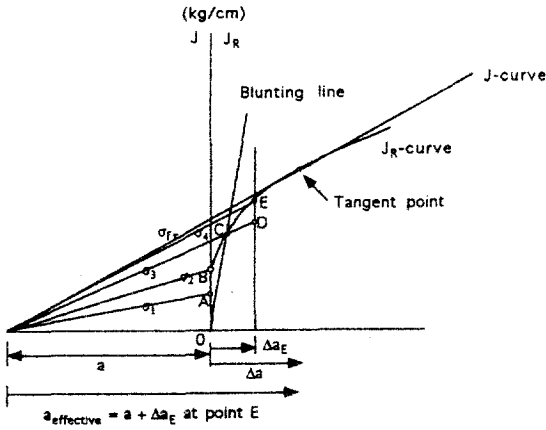


Fig. 4. Combined graph of the J-curve, and the crack tip blunting line.

point C. This crack proceeds as a stable fracture to point D. Therefore, the stress is increased from σ_3 to σ_4 in order for the crack to propagate. During the process of the stress increasing from σ_3 to σ_4 , the crack propagates in a stable fashion. When the stress reaches a fracture stress σ_{fr} , where $J=J_R$ and the J-curve becomes tangent to the J_R -curve, $dJ/da=dJ_R/da$, the fracture becomes unstable. After the tangent point, J is always bigger than J_R , there is unstable fracture. Crack propagation is fast, resulting in complete fracture. The stress at the initial crack propagation is σ_3 in Fig. 4. The stress at the initial crack propagation is expressed as σ_i . If at any time between σ_i and σ_{fr} the structure were to be unloaded, it would stay intact. In most cases, the difference between σ_i and σ_{fr} at instability is very small, and solving eq. (6) for σ_i may be adequate. Therefore, the stress at initial crack growth, σ_i , will be calculated in this study.

1.1.5 Calculation of the geometry factor H at the initial crack propagation

After calculation of J_{ic} , the stress at the initial crack propagation σ_i can be calculated from eq. (6) if the H value is already known for a given material from previous research. If geome-

try factor H is not known, H can be obtained by two methods. The first method is using non-linear Finite Element Analysis (Broek, 1989) on the cracked structure to get the plastic term of strain energy release rate $J_{plastic\ FEA}$. Then H can be calculated from the following equation that is derived from the $(H\sigma^{n+1}a/F)$ term of eq. (6). Namely, $H=(F \cdot J_{plastic\ FEA})/(\sigma^{n+1}a)$.

In this study, geometry factor H is determined by a second method. After the crack propagation, the crack length is changed to an effective crack length. The effective crack length, $a_{effective}$, is calculated from the measured crack length with LISA. The initial stress, σ_i , at the crack initiation is obtained from the intercept of J_R -curve and the blunting line. Every parameter of eq. (6) is known at the crack initiation except the geometry factor H. Then H can be calculated.

2. MATERIALS & METHODS

Double-edge notched samples are used as described in previous work (Park & Thorpe, 1996). Single-ply kraft sack paper is selected as a tough paper grade with an area of observation of $5\text{cm} \times 10\text{cm}$. Samples with initial crack-lengths of 0.0, 0.5, and 1.0 cm were tested for each specimen.

In the following sections, experimental procedures to construct the J- and J_R -curves are described. After constructing J- and J_R -curve, the fracture resistance and stress at initial crack propagation are calculated.

2.1 Calculation of stress-strain curve parameters n and F

Material constant n and pseudo-plastic modulus F are obtained from the relationship between stress and strain of kraft sack paper as a form of Ramberg-Osgood stress-strain equation by the following procedure.

Total strain, ϵ , is measured and elastic strain, $\epsilon_{elastic}$, is calculated from the relationship of ϵ_{elas}

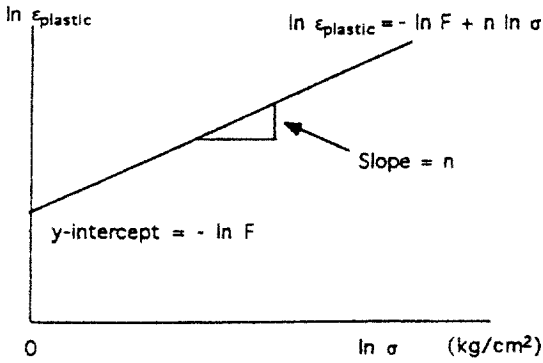


Fig. 5. Linear equation of $\ln \sigma$ and $\ln \epsilon_{\text{plastic}}$ to get n and F values.

$\epsilon_{\text{plastic}} = \sigma/E$. Plastic strain, $\epsilon_{\text{plastic}}$, is calculated by subtraction $\epsilon_{\text{plastic}} = \epsilon - \epsilon_{\text{elastic}}$. To calculate stresses, the cross sectional area of paper is obtained by multiplication of TAPPI standard thickness and ligament length. Ligament length is obtained by subtracting initial crack length, a , before crack propagation from the width of total sample, w .

F and n values are calculated with the natural logarithm from the equation $\epsilon_{\text{plastic}} = \sigma^n/F$, which becomes $\ln \epsilon_{\text{plastic}} = n \ln \sigma - \ln F$ (7). The slope of the linear equation (7) gives the n value at the slope and the F value as the intercept as shown in Fig. 5.

2.2 Fracture resistance, J_R , measurement

J_R is calculated from the area under the load-elongation curve, divided by the specimen's TAPPI thickness and ligament length. $J_R = (2 \times \text{Area under the load-elongation curve}) / (\text{thickness} \times \text{ligament length})$. Where, thickness = initial thickness of paper, and ligament length = total sample width $- 2 \times$ initial crack length = $w - 2a$.

2.3 Measurement of effective crack length, $a_{\text{effective}}$, to make the J_R -curve

The effective crack length is calculated by taking the initial crack length, plus half the size of plastic zone, $a_{125\%}$, that has a strain of 125% of failure strain. After crack propagation

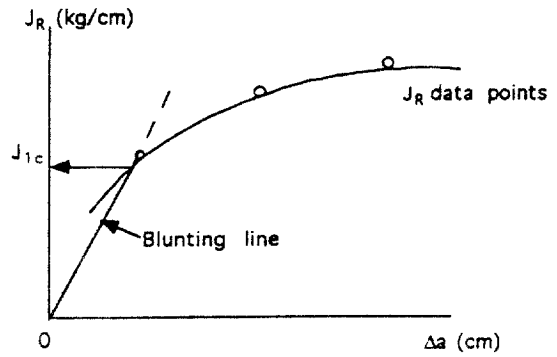


Fig. 6. J_{1c} calculation.

begins, the initial crack length, a , is incremented to an effective crack length, $a_{\text{effective}}$. The effective crack length was derived by Irwin to account for strain hardening (Irwin, 1958-1960) of elastic-plastic materials. The effective crack length is a sum of initial crack length and radius of plastic zone, r_p^* , as shown in Fig. 3.

Twice of the plastic zone radius, r_p^* , is equal to the crack length measured experimentally, $a_{125\%}$. The theoretical terms developed in fracture mechanics have been arbitrarily forced to equal the experimental results from LISA. $a_{\text{effective}} = a + (\frac{1}{2})(a_{125\%})$.

2.4 Calculation of geometry factor, β

Geometry factor β , which is a function of initial crack length, a , and width, w , of the sample, is calculated from the following equation $\beta (a/w) = Y / \sqrt{\pi}$. Where the Y value is obtained from $Y = 1.99 + 0.76(a/w) - 8.48(a/w)^2 + 27.36(a/w)^3$. For the range of a and w in this study, Y turns out to be close 2.00, and β becomes 1.13.

2.5 Calculation of fracture resistance J_R as J_{1c} and the initial stress, σ_1 , at initial crack propagation

J_R at crack initiation, J_{1c} , is obtained from the J_R data that depends on the propagation length of the crack, Δa , and the crack tip blunting line. The blunting line is given as $J_R = 2 \sigma_{ys} \Delta a$ (8). Where, σ_{ys} = yield stress = yield load, and Δ

a = propagation length of crack = $a_{\text{effective}} - a$.

The crack blunting yield stress is not obvious for most paper stress-strain curves, and so the 0.2%-offset, a rule of thumb, is used to establish yield stress.

As shown in Fig. 6 the J_R -curve and the blunting line intercept yields the J_{Ic} value and the propagation length of crack, Δa , at crack initiation. With known Δa , the initial stress, σ_i , can be obtained by interpolation of stress and the propagation length of crack, Δa , relationship at the initial crack propagation. Therefore, from eq. (6), the geometry factor H is calculated at that stage. The geometry factor H is dependent on the geometry of specimen.

3. RESULTS & DISCUSSION

3.1 Results

3.1.1 Stress and strain and the fracture resistance, J_R , of kraft sack paper

The stress and strain relationship can be expressed in a form of Ramberg-Osgood equation for kraft sack paper. Young's modulus and pa-

rameters of the stress-strain relationship are summarized in Table 1.

The fracture resistance, J_R , is measured from two tensile tests with initial crack lengths of 0.0, 0.5, and 1.0 cm throughout a sequential tensile load, but only fracture resistance at failure is summarized as shown in Table 1. The intercept of the J_R -curve and the blunting line at the initial crack propagation yields the fracture resistance, J_{Ic} . With known effective crack length, $a_{\text{effective}}$, the initial stress, σ_i , can be obtained from the effective length and the stress curve at the initial crack propagation.

The fracture resistance, J_{Ic} , the initial stress, σ_i , and the geometry factor, H , at the crack initiation is summarized in Table 2.

3.2 Discussion

Historically the load-elongation curve of paper has been described as elastic-plastic without further clarification. The obvious plastic portion of the curve was often ignored because it was difficult, perhaps impossible to explain in terms of mechanism or changes within the pa-

Table 1. Young's modulus, E , the stress-strain parameters, n , F , and the fracture resistance, J_R , at failure of samples.

	Crack length (cm)	E (kgf/cm ²)	n (unitless)	F (kgf/cm ²) ^{n}	J_R at failure (kgf/cm)
Cross-machine direction sample					
Replication 1	0.0	22,300	5.46	2.18×10^{14}	223.5
Replication 2	0.0	20,200	3.31	2.02×10^9	231.7
Replication 1	0.5	30,500	2.97	7.74×10^8	136.3
Replication 2	0.5	28,500	2.60	1.10×10^9	132.5
Replication 1	1.0	35,500	2.68	3.92×10^8	86.7
Replication 2	1.0	37,000	3.06	2.71×10^9	81.2
Machine direction sample					
Replication 1	0.0	51,800	1.94	3.40×10^7	155.3
Replication 2	0.0	42,200	3.01	1.92×10^{10}	115.6
Replication 1	0.5	59,400	3.68	2.03×10^{12}	83.0
Replication 2	0.5	55,400	3.65	1.57×10^{12}	88.1
Replication 1	1.0	73,100	3.59	2.09×10^{12}	65.2
Replication 2	1.0	75,200	3.74	6.49×10^{12}	65.8

Table 2. The crack propagation length, the fracture resistance, the initial stress, and the geometry factor at the crack initiation.

	a (cm)	Δa (cm)	J_{ic} (kgf/cm)	σ_i (kgf/cm ²)	H (unitless)
Cross-machine direction sample					
Replication 1	0.5	0.540	59.18	184	41
Replication 2	0.5	0.380	50.90	179	44
Replication 1	1.0	0.050	8.66	106	208
Replication 2	1.0	0.050	7.07	103	216
Machine direction sample					
Replication 1	0.5	0.002	1.58	69	14220
Replication 2	0.5	0.002	1.74	70	12800
Replication 1	1.0	0.002	2.22	90	8910
Replication 2	1.0	-	-	-	-

per. Linear image strain analysis allows a detailed analysis of the deformation within the paper throughout tensile loading to failure. Combining the experimental strain analysis with elastic-plastic fracture theory provides a reliable description of the load-elongation of paper.

The fracture mechanics approach to understanding the stress-strain behavior of paper has many advantages. First and foremost, it allows an engineering approach to quantify material parameters for paper. The strain energy release rate, J , the fracture resistance, J_R , the fracture resistance at crack initiation, J_{ic} , and the stress at initial crack propagation, σ_i , can be assigned definite numerical values. Secondly the engineering approach will allow the practical papermaker to quantify specific parameters in any grade of paper examined and then evaluate changes in furnish, paper machine modification, time, temperature, humidity, or any other variables. With use of the fracture mechanics paper should move closer to being a material with well defined engineering parameters. Application of the J and J_R -curves will allow a quick and easy approach to understanding the stress-strain behavior of paper that can be carried out in every paper mill.

Slow stable crack growth is an important fact of the load-elongation behavior of all tough papers. Linear image strain analysis defines crack growth. Understanding and appreciating that crack growth in every grade of paper will allow the practical papermaker to improve and adapt each paper to its end use.

3.2.1 Stress-strain relationship of tough paper

In Table 1, Young's modulus, stress-strain parameters, n , F , and the fracture resistance, J_R , at failure are summarized for changing initial crack length, a . Young's modulus of machine direction samples is higher than that of cross-machine direction samples. The Young's modulus is also increased with increasing initial crack length.

If we assume that paper follows the Ramberg-Osgood stress-strain equation, the material response of paper can be predicted with tensile experiments. Fluctuation of n and F has been shown to be acceptable, or perhaps expected in metals (Broek, 1989). Often the combined values of σ^n/F tend to cancel the individual fluctuations of n and F . Again, theory only approximates initial experimental results. The fracture resistance, J_R , at failure is larger in

cross-machine direction sample than in machine direction sample. The fracture resistance, J_R , also decreases when the initial crack length is longer.

3.2.2 Fracture resistance, J_R as J_{Ic} , initial stress, σ_i , and geometry factor, H , at initial crack propagation

In Table 2, the crack propagation length, Δa , the fracture resistance, J_R as J_{Ic} , initial stress, σ_i , and geometry factor, H , at initial crack propagation are summarized. In the technical literature, observation of the crack tip blunting phenomenon within a sample has been difficult or impossible. Crack tip blunting was very sensitive to small crack propagation within a short period of time. Using LISA, crack tip strains can be directly observed. Crack tip blunting is shown in previous work (Park, 1993). The crack tip blunting can be analyzed by a Δa value in this study.

The initial stress at the initial crack propagation is summarized in Table 2. The initial stress at the crack propagation is greater in the cross-machine direction sample than in the machine direction sample.

4. CONCLUSION

Elastic-plastic fracture mechanics (EPFM) has been applied to the tensile analysis of paper. Many of the fracture mechanics' parameters can be calculated from the dynamic strain profile using linear image strain analysis (LISA). Those parameters allow the material properties of paper to be quantified during tensile failure.

The theory of fracture mechanics is evolving and its application to the tensile failure of paper is just beginning. Experimental techniques to quantify what is termed elastic-plastic strain to failure may now be ahead of the theory. Plastic zones can now be fully quantified in terms of local strain intensity and direction. The crack propagation, Δa , is obtained by lin-

ear image strain analysis (LISA). The first experimental measurements of crack propagation in paper have been combined with fracture mechanics theory. This attempt to fit experimental results to existing theory should be considered embryonic, but promising. The theory will change and the experimental results will improve with replication.

Elastic-plastic stable fracture propagates if the strain release rate, J , equals the fracture resistance, J_R . If the strain release rate, J , equals the fracture resistance, J_R , and the slope of the strain release rate is tangent to the fracture resistance curve, $dJ/da = dJ_R/da$, then unstable fracture occurs. By using the energy criterion, the stress at the initial crack propagation, the fracture resistance, the crack propagation length, and the geometry factor can be determined. These parameters define the toughness of a material.

Fracture mechanics allows an engineering approach to quantifying material parameters for paper. Understanding of the fracture behavior will provide parameters which can be used as a tool to improve paper to its end use.

REFERENCES

1. Broek, D. 1986. Elementary Engineering Fracture Mechanics, 4th ed. Kluwer Academy Pub.
2. Broek, D. 1989. The Practical Use of Fracture Mechanics, Kluwer Academy Pub.
3. Choi, D., and J. Thorpe. 1992. Progressive deformation at the crack tip in paper during mode I fracture. - Part I. bond paper-. *Tappi* 75(10) : 127~134
4. Choi, D., J. Thorpe, and R. Hanna. 1991. Image analysis to measure strain in wood and paper. *Wood Sci. & Tech.* 25 : 251~262
5. Irwin, G. R.. 1958. Fracture, Handbuch der Physik VI. Flgge Ed., Springer : 551~590
6. Irwin, G. R.. 1960. Plastic zone near a crack and fracture toughness, Proc. 7th

7. Kumar, V. *et al.* 1981. An Engineering Approach for Elastic-Plastic Fracture Analysis. Electric Power Res. Inst. NP-1931
8. Park, J.-M. 1993. Study of yield and fracture of paper. Ph. D. Thesis. College of Environmental Sci. & Forestry, State Univ. of New York
9. Steadman, R., and C. Fellers. 1986. Measuring fracture strength of tough papers. *In* Solid Mechanics Advances in Paper Related Industries. Proceeding of 1986 NSF Workshop
10. Steadman, R. and C. Fellers. 1987. Fracture toughness characterization of papers at different climates. International Paper Physics Conference Proceedings CPPA. Montreal, Canada
11. 박종문 · J. Thorpe. 1996. 상업용지의 Mode I 파괴연구. 펄프 · 종이기술 28(4) : 17~30